Beta decay studies with total absorption spectroscopy and the *Lucrecia* spectrometer at ISOLDE

OPEN ACCESS
IOP Publishing

Made open access 7 August 2017
Journal of Physics G: Nuclear and Particle Physics

J. Phys. G: Nucl. Part. Phys. **44** (2017) 084004 (25pp) https://doi.org/10.1088/1361-6471/aa797f

Beta decay studies with total absorption spectroscopy and the *Lucrecia* spectrometer at ISOLDE*

B Rubio[1], W Gelletly[1,2], A Algora[1,3], E Nacher[4] and J L Tain[1]

[1] IFIC (CSIC-Univ. of Valencia), E-46980 Paterna, Spain
[2] Department of Physics, University of Surrey, Guildford, Surrey GU2 7XH, United Kingdom
[3] Institute of Nuclear Research of the Hungarian Academy of Sciences, Debrecen H-4026, Hungary
[4] Instituto de Estructura de la Materia, CSIC, E-28006,Madrid, Spain

E-mail: berta.rubio@ific.uv.es

Received 10 December 2016, revised 8 April 2017
Accepted for publication 14 June 2017
Published 30 June 2017

Abstract

Here we present the experimental activities carried out at ISOLDE with the total absorption spectrometer *Lucrecia*, a large 4π scintillator detector designed to absorb a full gamma cascade following beta decay. This spectrometer is designed to measure β-feeding to excited states without the systematic error called *Pandemonium*. The set up allows the measurement of decays of very short half life. Experimental results from several campaigns, that focus on the determination of the shapes of β-decaying nuclei by measuring their β decay strength distributions as a function of excitation energy in the daughter nucleus, are presented.

Keywords: beta decay, strength functions, total absorption gamma spectroscopy, nuclear shapes

(Some figures may appear in colour only in the online journal)

1. Introduction

Beta decay is the most common mode of radioactive decay for unstable nuclei. It is a process that is well understood. Studies of β-decay are important because they provide information on both nuclear structure and nuclear astrophysics. This information is also of importance for some applications, particularly those related to the fission process since, in general, the

* This article belongs to the Focus on Exotic Beams at ISOLDE: A Laboratory Portrait special issue.

products of fission decay by beta emission. Thus, it is important for an understanding of radioactive decay heat since 7%–8% of the reactor power is generated in the decay of the fission products [1]. Reactors are intense sources of antineutrinos because of these beta decays, with a typical intensity of $\sim 2 \times 10^{19}$ antineutrinos per second. As a result they are of considerable interest for studies of neutrino oscillations (Double Chooz [2], Daya Bay [3] and Reno [4]).The antineutrino spectrum is also sensitive to the mixture of fuel in the reactor. Accordingly it is proposed that each reactor might have a relatively small antineutrino detector placed close to it in order to monitor the reactor fuel content to ensure that it is not being manipulated to produce material for weapons [5]. In terms of nuclear structure one important quantity to be determined is the beta strength function, or the directly related quantity Fermi or Gamow–Teller beta-strength, B(F) or B(GT), because it relates to the transition matrix elements between the ground state of the parent nucleus and the excited states in the daughter nucleus. The two quantities are defined as follows

$$B(\mathrm{GT}) = |\langle \Psi_f | \sum_{\mu} \sum_{k} \sigma_k^{\mu}\, t_k^{\pm} | \Psi_i \rangle|^2, \tag{1}$$

$$B(\mathrm{F}) = |\langle \Psi_f | \, t^{\pm} | \Psi_i \rangle|^2, \tag{2}$$

where σ and t are the beta decay operators that can change the nuclear spin and the isospin by one unit. The same quantity, from the experimental point of view has a very different form,

$$B(\mathrm{GT})^{\beta} = \frac{K}{\lambda^2} \frac{I_{\beta}(E)}{f(Q_{\beta} - E, Z) T_{1/2}} = \frac{K}{\lambda^2} \frac{1}{ft}, \tag{3}$$

$$B(\mathrm{F})^{\beta} = \frac{K}{(1 - \delta_c)} \frac{I_{\beta}(E)}{f(Q_{\beta} - E, Z) T_{1/2}} = \frac{K}{(1 - \delta_c)} \frac{1}{ft}, \tag{4}$$

where $K = 6143.6(17)$ s, $\lambda = g_A/g_V = -1.270(3)$ and δ_c is the Coulomb correction factor. $I_{\beta}(E)$ is the β-feeding, f is the Fermi function, Q_{β} is the β-decay Q value or energy available in the daughter nucleus, and $T_{1/2}$ is the β-decay half-life.

Consequently, if we are to deduce the beta strength function one must measure three quantities: $T_{1/2}$, Q_{β} and the direct population in beta decay of all the individual states in the daughter nucleus. It is not straightforward to measure this quantity since the individual transitions do not have discrete energies as is the case in alpha and gamma decay. Each beta spectrum takes a continuous form because the energy released is shared between the β particle and a neutrino/antineutrino. In general the approach is to determine the feeding for individual levels indirectly from the difference in the sum of the intensities of all the gamma rays feeding a level and the corresponding sum of the intensities of all those de-exciting it.

The root of the problem of measuring the β feeding lies in the fact that most studies of this kind rely on the use of the ubiquitous Ge detectors. They are ideally suited to the kind of multiple coincidence studies needed to establish level and decay schemes. In general, however, even in the form of large arrays of detectors they have limited detection efficiency and the efficiency has a strong dependence on the γ-ray energy. As a consequence there is a significant probability that a γ ray is not observed in the spectrum. We are then unable to tell whether it does not exist or whether it lies below the detection sensitivity level at that energy. It is obvious that in such a measurement we may be unable to measure the direct feeding to a level in β decay because of the energies of the γ rays involved and the fragmentation of both the feeding in β decay and the γ de-excitation of the levels. In other words our measures of the balance of feeding and de-excitation will become inaccurate. Looked at overall this means that some real feeding to higher excited states is shifted systematically to become apparent

feeding to levels at low excitation energy. When the Q window in β decay becomes large, as it does when we move away from the valley of nuclear stability, this effect will be even more evident because the nuclear level density increases rapidly with excitation energy. There is then, in general, a greater fragmentation of the beta decay feeding. This source of systematic error has come to be known as the *Pandemonium* effect [6].

Can this problem be overcome? One way is to adopt an entirely different approach, such as total absorption (gamma-ray) spectroscopy (TAS)[5]. Here the aim is to measure the beta feeding of the levels directly rather than detecting the individual gamma rays. In principle, this can be done by detecting all of the gamma rays emitted in the cascades de-exciting the state with a spectrometer that is 100% efficient. In practice 100% efficiency is not practicable. The problem then reduces to the question of whether, given a detector with a geometry as close to 4π as possible and a good intrinsic efficiency (this eliminates the Ge crystal option), we can extract the beta feeding up to the excitation energy in the daughter nucleus allowed by the Q window.

It turns out that the answer is yes but it not only requires a very large detector but also both minimising the dead material which can cause partial absorption of the cascades and sophisticated analysis techniques. In what follows we shall first look at how this method of determining the beta strength function has developed over the years in section 2. We shall also see how the analysis of the spectra from TAS has developed in section 3.1. We then turn to the main subject of this article, namely the *Lucrecia* spectrometer installed at CERN-ISOLDE in section 3.

2. The history

In the early 1970s, β-decay studies were made for quite large numbers of unstable nuclei with the TAS technique, both at ISOLDE [7] and OSIRIS [8]. In both cases, the basic spectrometer consisted of two cylindrical NaI detectors of 15 cm diameter and 10 cm length with the radioactive source on the central axis between the two counters. There was an aperture between the two crystals which allowed for the introduction of a ring of plastic scintillator for beta detection in the experiments at OSIRIS. The authors of these papers described their method as involving 'incomplete total absorption'. They devoted considerable effort to analysing the spectra. Already they pointed out the main difficulties in the analysis of the data and used Monte Carlo simulations to construct their response functions. Stimulated by Hardy *et al*'s discussion [6] of the difficulties in measuring beta strength functions and the high-resolution experiments of Firestone [9], Alkhazov used a spectrometer consisting of two NaI crystals (one 20 cm diameter and 20 cm length with a well of 4 cm in the middle to host the radioactive sample and a Silicon detector and a second NaI detector of 20 cm diameter and 10 cm length), hereinafter referred to as the Russian TAgS, to examine the beta decays of several nuclei [10]. Their conclusion chimed with that of Hardy *et al* that most such decay schemes were substantially incomplete and the log *ft* values derived from them unreliable. The next significant step forward was made in the 1990s by Greenwood *et al* [11], who used a large, 25.4 cm diameter and 30.5 cm long NaI well counter, to measure beta strength functions for a range of separated fission fragments from a ^{252}Cf source. These authors analysed the data by simulating the entire decay scheme using Monte Carlo methods. They also discussed

[5] We note here that we will use the same name, total absorption spectroscopy (TAS) for the technique as for the apparatus itself, total absorption spectrometer (TAS). Although the technique is designed for the total absorption of γ rays, it is unavoidable that the spectrometer will also be sensitive to the penetration of the beta particles as well as to the penetrating neutrons.

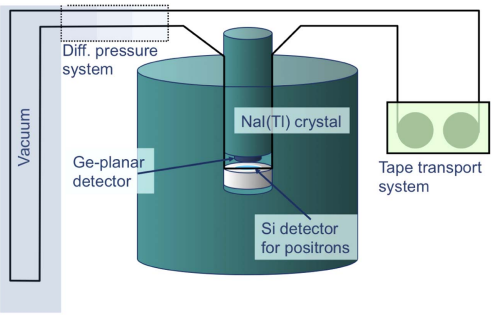

Figure 1. A schematic diagram showing the GSI-TAS [13, 14] and the arrangement of its ancillary detectors. Reprinted figure with permission from [14], Copyright (2016) by the American Physical Society.

many of the inherent difficulties in the analysis. Some of the cases measured by Greenwood *et al* have been remeasured recently and analysed with a more sophisticated system [12]. The new results confirm the results of Greenwood *et al* showing that this detector was sufficiently large to be a good spectrometer and that the analysis of the data was carried out with care.

At the end of the 1990s another large single crystal, closer to the 'ideal', 4π full efficiency spectrometer was constructed at Berkeley and then transported and installed at the GSI on-line mass separator [13], where it was used very successfully for about one decade before being returned to Berkeley following the premature closure of the mass separator. It consisted of a single, very large cylindrical crystal of NaI(Tl) of 35.6 cm diameter and 35.6 cm length with a well on the central axis that could be filled by a matching plug of NaI, see figure 1. The setup included a small Ge detector and two thin ΔE detectors of Si that could be placed in the well close to the radioactive source for the purpose of recording coincidences between the TAS and betas and x-rays. The activity from the mass separator was implanted in a magnetic tape that could be moved to carry the activity to the centre of the crystal and at the same time remove residual daughter activity. Equally important was the development at Valencia of the computer programs needed to provide consistent and reliable analysis of the data acquired with the spectrometer. This involved finding a solution [15, 16] to the inverse, ill-posed problem that is described later in this article in section 3.1, taking account of the nonlinearity of the light output in the scintillator [17] and the pile-up in the electronic circuits [18].

Figure 2 compares the B(GT) distribution for the decay of ^{156}Tm measured with the Russian TAgS and the GSI spectrometer. In both cases the Gamow–Teller resonance is clearly seen.The spectrum from the GSI spectrometer was analysed using the techniques developed at Valencia. The summed B(GT) measured with the two spectrometers was the same, namely 0.48 $g_A^2/4\pi$, but one can see that the combination of a superior detector and improved methods of analysis shows more detailed structure in the resonance.

It is not appropriate here to discuss all of the work carried out with this spectrometer at GSI. Instead we will briefly mention two works of interest (which are also related to the research of the co-authors of the present article) that stimulated the acquisition and setting up of the *Lucrecia* spectrometer at ISOLDE. In the first of them Algora *et al* [19] studied the gamma-ray spectrum from the decay of the ^{150}Ho 2^- state with the CLUSTER CUBE Ge array [20], which consisted of six EUROBALL clusters [21] in compact geometry. This array had the equivalent of 42 individual Ge detectors. It had a detection efficiency of 10.2(5)% at a gamma-ray energy of 1332 keV. This work was important because it used for the first time the most advanced Ge detectors to study a complex beta decay. Previous works were carried out

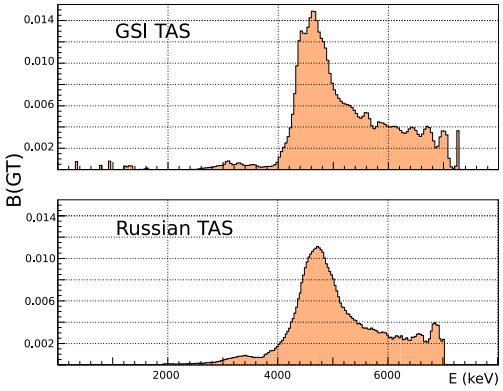

Figure 2. The figure shows the B(GT) distribution for the decay of ^{156}Tm measured with the GSI-TAS (upper half) and the Russian TAgS (lower half), see text.

with a couple of Ge detectors of modest efficiency with the rationale that one can increase the solid angle by moving the detectors closer to the radioactive sample, but this has the unfortunate consequence that summing of cascade γ rays occurs in the detector. This experiment demonstrated the advantages of having increased coincidence capabilities as well as the possibility of using add-back mode for detecting high energy gamma-rays. Figure 3 shows the beta strength as a function of excitation energy in the daughter nucleus following the beta decay of the 2^- ground state of ^{150}Ho to levels in ^{150}Dy measured with the CLUSTER CUBE (in green) where 1064 gamma-ray lines were observed that were fitted into a decay scheme with 295 levels in ^{150}Dy. In other words one could think that this experiment provided a 'relatively complete' decay scheme for ^{150}Ho. The same decay was studied with the GSI TAS. The results are also shown on the figure (red filled curve). One can clearly see how the Ge arrays lose sensitivity as a function of excitation energy in the daughter nucleus as compared with the TAS results. Once converted into B(GT) strength we conclude that we lose about 50% of the total strength when compared with the TAS measurement. However the higher resolution measurements were essential to obtain the details of the level scheme in the daughter nucleus, such as the distribution among the possible spins, and the fine structure of the resonance.

The second work concerns the beta decays of a number of rare-earth nuclei [14]. In the β^+-decay of nuclei with $Z < N$, Fermi transitions are forbidden and GT transitions are, in general, severely hindered because in transforming the available protons into neutrons the corresponding allowed orbitals for neutrons are occupied. There are some exceptions such as the $N \sim Z$ nuclei with $A \sim 80$ where the protons and neutrons fill orbitals with the same quantum numbers. It is also possible when the protons are filling a $J>$ orbital and the corresponding $J<$ orbital is empty on the neutron side. This occurs for the nuclei near ^{100}Sn [22] where the protons in the intruder $g_{9/2}$ orbital decay to the empty or partially occupied $g_{7/2}$ neutron orbital. It also happens for the rare-earth nuclei above ^{146}Gd, where the intruder $h_{11/2}$ orbital is being filled with protons that can decay to the empty $h_{9/2}$ neutron orbital. The latter situation was examined in a series of measurements on the rare-earth nuclei [21]. The resulting B(GT) distributions are summarised in figure 4. The GT resonance which was observed a long time ago in charge exchange reactions on stable nuclei and lies at high excitation energy in the final nucleus, was clearly observed for the first time in the beta decay of the two Ho and Tm isotopes at 4.5 MeV. Moreover a possible source of the long standing

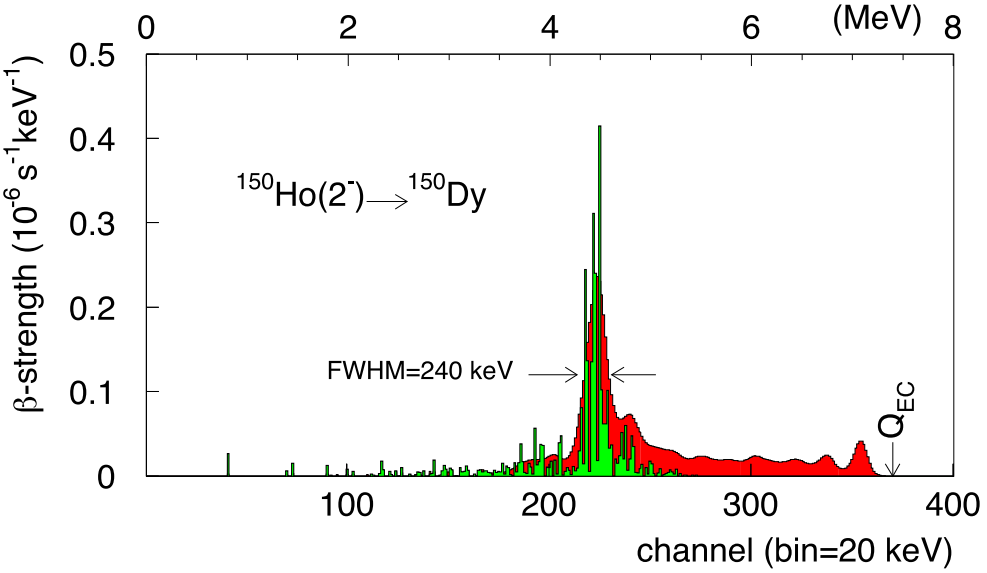

Figure 3. The B(GT) distribution for the decay of the 2^- state in ^{150}Ho to levels in ^{150}Dy with the CLUSTER CUBE [20] and the GSI-TAS [13], see [19]. Reprinted figure with permission from [19], Copyright (2003) by the American Physical Society.

problem of the GT quenching, discussed in charge-exchange reactions for more than three decades, namely the hidden strength in the tail of the resonance at high energies was clearly observed here, thus avoiding the background ambiguities associated with the reactions. Possible sources of the GT quenching were discussed in detail.

All in all the GSI-TAS was very successful. The main limitation to its use was the fact that the nuclei of interest had to be produced in fusion-evaporation reactions. Roughly speaking this was the point where it was decided to install *Lucrecia* at ISOLDE, where the use of spallation and fission of heavy targets with high energy protons means that a wide range of species were produced with high intensity. At the same time other unwanted species are also produced and one must use a variety of techniques to 'clean' the beam as well as using coincidences with x-rays to focus on the electron capture component of beta decays when possible. The success of the GSI-TAS had shown that a rich source of information was there to be mined and it prompted the building of *Lucrecia*, which will be described in detail in the next section.

More recently several new spectrometers have been designed and commissioned. All of them are segmented, a feature introduced to allow one to make use of the information obtained on the gamma-ray multiplicity in the analysis. *Rocinante* [24, 25] a compact, modular spectrometer made of twelve BaF_2 crystals was the first segmented TAS detector designed for β-decay studies. It consists of twelve BaF_2 optically independent crystals arranged in a prism geometry of 25 cm width and 25 cm length. It has a longitudinal hole of diameter 55 mm along its central axis. Each BaF_2 detector is optically isolated by means of a thin reflecting wrapping and is viewed by a single 3 inch photomultiplier tube (see figures 5 and 6). Simulations indicate a gamma-ray efficiency of ∼80% at 5 MeV for single gamma rays. A Si detector can be placed at the measuring point, inside the TAS, to detect β particles. BaF_2 has the intrinsic disadvantage of being contaminated with Radium, which is alpha active. This can be turned into an advantage by using it for continuous monitoring of the

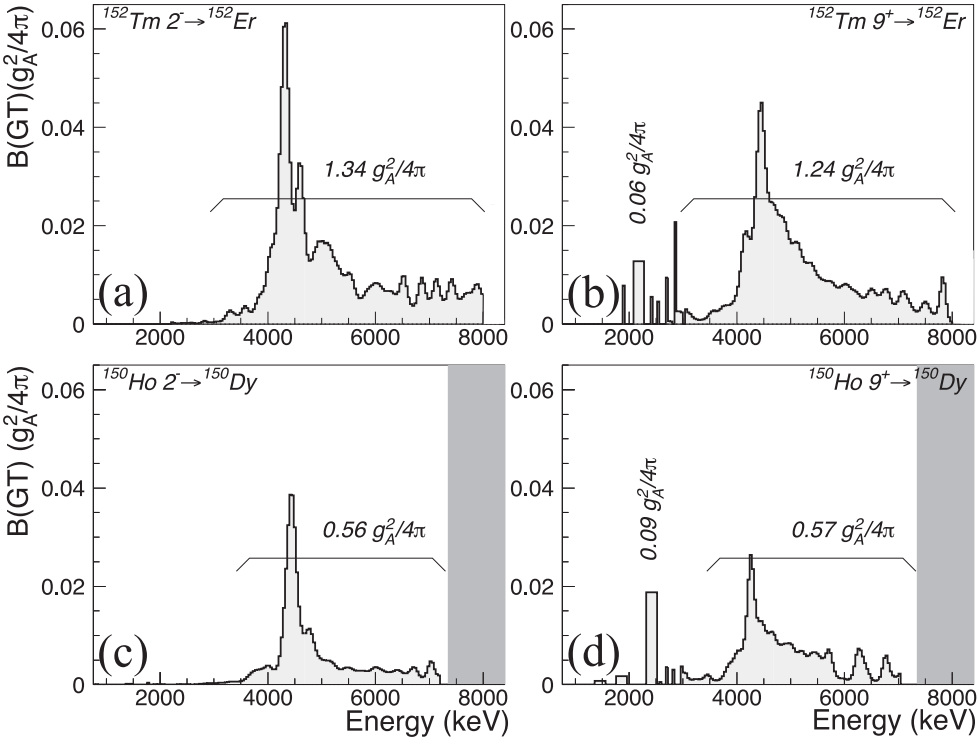

Figure 4. B(GT) distributions from the β decay of Tm and Ho $N = 83$ isotopes measured with the GSI-TAS [14]. The GT resonance is clearly seen. One can also see how the strength extends up to the available energy window determined by the Q value (grey area indicates excitation energies beyond the Q value). Reprinted figure with permission from [14], Copyright (2016) by the American Physical Society.

energy gain in the spectrum of the individual detectors. The identification of the alpha peaks allows the continuous correction of small gain changes in the measured spectra. One advantage compared with other scintillators is that it has relatively low sensitivity to neutrons. Advantage has been taken of this to study a number of β-delayed neutron emitters [25]. *Rocinante* has been used successfully in a number of experiments [23, 24].

The DTAS spectrometer [26] was designed specifically, as part of the DESPEC setup [27] at the future FAIR facility in order to take advantage of the possibility of studying short-lived β decays produced in the fragmentation of relativistic heavy ion beams. In the design study for this spectrometer Monte Carlo simulations and experiments were undertaken to ensure that the spectrometer satisfied the main criteria of a TAS namely:

(i) The largest possible coverage of the solid angle in order to maximise the total detection efficiency,
(ii) A large detector thickness and a minimum amount of dead material to maximise the peak detector efficiency,
(iii) A reasonable energy resolution from 10 s of keV to 15 MeV, and
(iv) A minimum sensitivity to neutrons since studies of exotic, neutron-rich nuclei can involve β-delayed neutron emission.

Figure 5. A photograph of *Rocinante*, a TAS based on BaF_2 scintillators, see text.

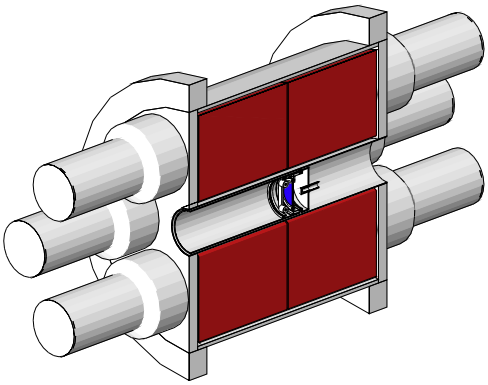

Figure 6. A longitudinal cut through *Rocinante* [25] showing the modular arrangement and the central through hole. Reprinted figure with permission from [25], Copyright (2017) by the American Physical Society.

Following extensive simulations two favoured solutions were investigated in detail, namely a modular array of one hundred and twenty eight 5.5 × 5.5 × 11 cm^3 crystals of $LaBr_3$(Ce) and separately a similar modular array consisting of sixteen 15 ×15 × 25 cm^3 NaI (Tl) crystals. This despite the fact that both materials are hygroscopic. The advantages and disadvantages of the two possibilities were explored in detail with the final decision being to build the spectrometer of NaI(Tl), see figure 7. This was partly due to the much higher cost of the $LaBr_3$(Ce) material. The geometry adopted for DTAS is shown schematically in figure 8 where we see the sixteen modules coupled to 5 in. photomultiplier tubes arranged around the central hole of 10 × 10 cm^2 that is needed to house AIDA [28], the array of DSSSDs placed at the end of the Super-FRS (GSI) [29] or BigRIPS (RIKEN) [30] to detect the separated, short-lived nuclei produced in fragmentation and recorded in coincidence with DTAS. The spectrometer has been commissioned [31] with radioactive species with the very clean beams from the double Penning Trap at the IGISOL on-line mass separator facility [32] at the University of Jyväskylä.

The SuN detector [33] was built at NSCL, Michigan for the purpose of studying (p, γ) and (α, γ) reactions of interest in various astrophysical scenarios. It consists of an eight-fold segmented cylinder of dimensions 16 in. long by 16 in. diameter made of NaI(Tl). The

Figure 7. A photograph of the DTAS [26] spectrometer.

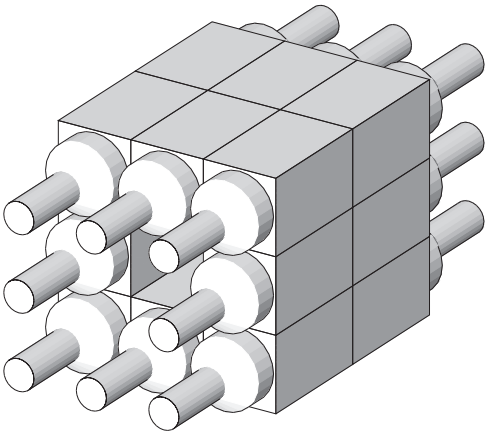

Figure 8. A schematic drawing of DTAS [26] showing the modular construction and central through hole to house AIDA [28]. Reprinted from [26], Copyright (2015), with permission from Elsevier.

cylinder is in two halves that fit around a 1.8 in. diameter hole that can house an accelerator beam line. Each half of the barrel is divided into four optically isolated sections separated by 0.5 mm of aluminium and 0.25 mm of reflecting material. Each of the eight segments is coupled to three photomultiplier tubes at equal angular spacing around the central beam line. The spectrometer is well designed for the purpose of studying capture reactions and it has been commissioned [33] at Notre Dame and applied at NSCL as a TAS [34].

Another new segmented detector was built at ORNL,Tennessee and is called MTAS [35]. It consists of nineteen NaI(Tl) detectors, each 21 in. long and hexagonal in shape with an approximate maximum diameter of 8 in. The central detector has a through hole of 2.5 in. diameter to accommodate a moving tape system that carries deposited activity from outside to the centre of the detector and two Si strip detectors for β coincidence studies. Since the strips are aligned at right angles to the tape the detector signals help to ensure that the source is located in the centre of the detector. The detector has been used for a number of applications [36]. In principle the degree of separation should help in the analysis. There are too few

results from this spectrometer as yet to tell how much of an advantage the large size and segmentation give.

3. *Lucrecia* at CERN-ISOLDE

Earlier it was pointed out that for the β^+-decays of nuclei with $Z \sim N$ and $A \sim 80$, GT transitions are, in general, not hindered because in these nuclei the protons and neutrons fill orbitals with the same quantum numbers. Together with the success of the GSI-TAS, the wide range of radioactive species available at ISOLDE, the development of consistent and reliable methods of data analysis and the possibility of studying nuclear shapes, motivated the acquisition of *Lucrecia* and its installation at CERN-ISOLDE.

The *Lucrecia* detector [38, 39] is slightly larger in size than the GSI-TAS (see figures 9 and 10). It is based on a cylindrical, single crystal of NaI(Tl) that is 38 cm in length and 38 cm in diameter with a 7.5 cm diameter through hole perpendicular to the central axis of the cylinder. The detector, shown in figure 11, is enclosed in an aluminium cylinder of 13 mm thickness that is reduced to 11 mm in the radial hole to minimise gamma-ray absorption. Good light reflexion is ensured by a coating of 2 mm Al_2O_3 on the inner surface of the aluminium cylinder. The through hole is an essential part of the design since it allows the separated activity to be deposited directly on a tape system at the centre of the detector. This eliminates the time delay due to carrying the activity from the ISOLDE separators, that has been implanted in a tape outside the detector, to the measuring point at the centre of the detector. This allows the study of the shortest lived activities available from ISOLDE. A set of three collimators (see figure 12), placed at 950, 975 and 992 mm from the collection point, limits the beam halo and forms a 6×8 mm^2 beam spot on the mylar tape at the centre of the NaI(Tl) crystal. Under these circumstances the tape system is used to carry away daughter activities rather than refresh the source of interest. When longer lived activities are studied the tape is used more conventionally to carry implanted activity into the spectrometer. The last section of the beam line that is inserted into the detector is a telescopic aluminium tube of 1.2 mm thickness, 68 mm diameter sealed with a kapton window (figures 9 and 12).

The through hole also allows one to place a number of ancillary detectors close to the counting position on the opposite side from the beam entrance, so that one can record coincidences between the γ-ray spectrum in *Lucrecia* and β particles, positrons, x-rays and γ-rays. For example in the measurements described below a 2 mm thick plastic scintillator sits close to the source position backed by a Ge telescope, consisting of a 1 cm planar detector and a 5 cm coaxial Ge detector behind it. Figure 12 shows schematically a horizontal cut of the experimental setup when the beam is implanted directly in the centre of the *Lucrecia* NaI(Tl) detector. As mentioned earlier in describing other detectors, background can be a problem and one might expect a mixed background of γ-rays and neutrons in the ISOLDE hall. Accordingly the detector is housed in shielding with four layers of material; 10 cm boron polyethylene, 5.1 cm lead, 1.5 cm copper and 2 cm of aluminium. The overall weight is 11 tons. Monte Carlo simulations with the MCNPX 2.2.3 code suggest that the shielding efficiency of this system for slow ($E_n \sim 1$ eV) and fast ($E_n \sim 1$ MeV) neutrons is 100% and 90% respectively. Experimental observations are consistent with this. The counting rate in the TAS due to γ rays is reduced to 1 kHz with the shielding closed, a factor of 3.5 improvement compared with when it is open. The residual background is mainly due to the decay of the ^{40}K in the crystal. The temperature inside the closed shielding is maintained within a range of ± 0.50 °C using an industrial air conditioning unit. The figures 9 and 10 show the *Lucrecia* detector with the shielding open.

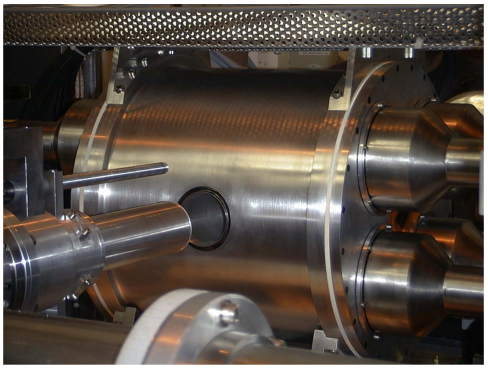

Figure 9. A photograph of the *Lucrecia* detector showing the through hole at right angles to the detector axis and the telescopic extension to the ISOLDE beamline withdrawn from the hole.

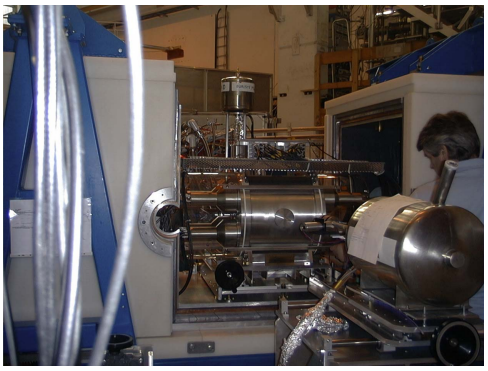

Figure 10. A photograph of the *Lucrecia* detector inside its shielding. The through hole, that houses the end of the beam line and the ancillary detectors, is clearly visible.

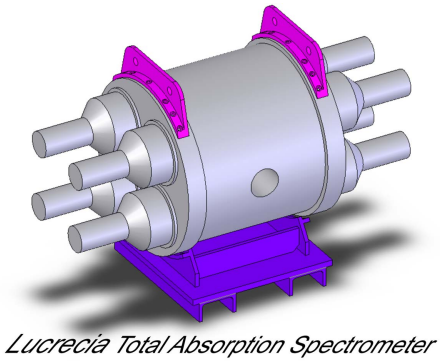

Figure 11. A schematic drawing of the Lucrecia detector. Reprinted figure with permission from [37], Copyright (2013) by the American Physical Society.

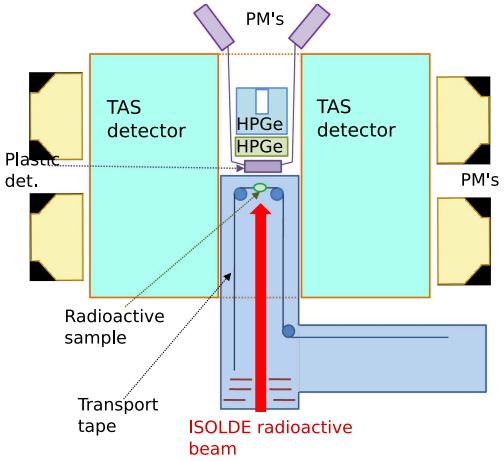

Figure 12. A cross-section through the Lucrecia setup at ISOLDE. Reprinted figure with permission from [37], Copyright (2004) by the American Physical Society.

Figure 13 shows the total and peak detection efficiencies for *Lucrecia* as a function of gamma-ray energy. There are slight differences between *Lucrecia* and the GSI-TAS or the DTAS. The slightly lower values for *Lucrecia* in comparison with the GSI-TAS are due to the through hole. A NaI(Tl) plug was manufactured for *Lucrecia* but is in general not used. As a result the efficiency for detecting individual gamma rays is smaller. For most real cases the multiplicity of gamma ray cascades is rarely 1 and the difference in total efficiency is much less. The energy resolution for *Lucrecia* is 7.1% and 5.4% at 662 and 1332 keV energy, respectively.

3.1. The analysis methods

The exploitation of *Lucrecia* would have been much more difficult without the development of analysis methods and techniques [15–18] that we will briefly summarise here before going on to discuss some examples of *Lucrecia* in use. Since real TAS spectrometers are not 100% efficient it is necessary to consider the response to beta particles and the electromagnetic de-excitation cascades in unfolding the measured spectra. It is necessary first to subtract contaminants in the spectra. One then begins with the relationship between the measured data d and the level feeding distribution f which can be represented by

$$d = R(B)f, \tag{5}$$

where R is the response function matrix of the spectrometer which depends on the γ decay branching ratio B of the levels populated in the daughter nucleus. This is a non-trivial exercise because this equation falls into the class of ill-posed problems and the solution is not straightforward. Tain and Cano-Ott [15, 16] devoted considerable effort to the possible solutions. The obvious first step is to construct the response function of the TAS used. It will be different on every occasion because of differences in the ancillary detectors and other experimental conditions as well as differences in the decay scheme. It includes the response of the apparatus to the different quanta and particles emitted in the decay as well as the de-excitation branching ratios for the levels populated in the daughter nucleus. Tain and Cano-Ott examined how sensitive the results were to different assumptions for the gamma-ray branching ratios. In some cases they are insensitive to the initial assumptions but in general

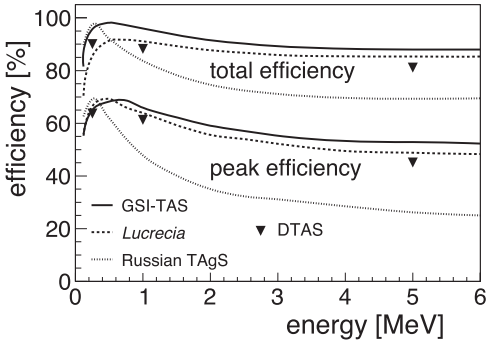

Figure 13. Total efficiency and peak efficiency for single γ rays measured with *Lucrecia* (ISOLDE), the GSI-TAS, the Russian TAgS and DTAS (NaI(Tl)).

not. In general one needs to have a solid knowledge of the level scheme at least up to some reasonable excitation energy, the cut-off energy, and complement this information with a good guess for the excitation energies above this. The nuclear statistical model based on average level densities and photon strength functions is used to obtain realistic branching ratios for the unknown part of the level scheme. As part of the optimisation procedure in the analysis, the cut-off energy and the parameters of the statistical model can be varied to test how robust the solutions are and provide a measure of the errors involved in the procedure. The methods they adopt also rely on Monte Carlo simulations of the response to individual single quanta, γ-rays, beta particles that enter the crystal etc. These authors have put the analysis of TAS data on a sound footing although in applying the methods due care and attention must be paid to the individual case. In addition to solving the 'ill-posed' problem the Valencia group also looked in detail at the effect of the nonlinearity in the light output of the scintillator [17] and of the pile-up in the electronic circuitry [18] and showed how they can be taken into account.

3.2. The measurement of nuclear shapes in beta decay; $N \sim Z$ nuclei

The simplest thing one can visualise about an atomic nucleus is its shape. Strangely enough it turns out that it is far from trivial to measure it. As with most systems of particles, no matter the forces between them, the default shape one expects is a sphere. In general terms we now have a picture of nuclei at or very near to closed shells that are spherical and as nucleons are added, even in quite small numbers, the shape becomes deformed. A long way from the Magic numbers the deformation becomes marked and many such nuclei are thought to be prolate or oblate spheroids. Other more complicated shapes are possible (see e.g. [40]). This very simple picture does not hold everywhere in the Segre chart and the example(s) we have chosen to illustrate the use of *Lucrecia* investigate the shapes of the $N \sim Z$ nuclei with $A \sim 80$ where (a) the shape can change dramatically with the addition or subtraction of a few nucleons and (b) states in the nucleus with very different shapes lie close to the ground state, in other words the phenomenon called 'shape coexistence' exists. There are reasons why the nuclei in this particular region exhibit this behaviour. Firstly the neutrons and protons are filling orbits with the same quantum numbers. Secondly they have a relatively low level density at low excitation energies. If we look at them in terms of mean field models [41, 42] we find that the single particle state diagram shows large energy gaps for protons and neutrons at $Z, N = 34, 36$ on the oblate side and 38 on the prolate side. Models of this kind do

indeed suggest the coexistence of states with quite different shapes in these nuclei. Prior to the experiments with *Lucrecia* described below there was already some experimental evidence to support this picture [43, 44] in the Se and Kr nuclei and it was also predicted for the lightest Sr nuclei.

The overall aim of the experiments was to map out the deformation of the Sr and Kr nuclei near the $N = Z$ line as a function of Z and N. A simple aim but there are obstacles. A number of methods of determining the ground state deformation in unstable nuclei do exist. They are based on the interaction of the electric quadrupole moment of the nucleus with an external electric field gradient [45–47]. However they do not apply to nuclei with $I = 0$ or $1/2$, thus ruling out experiments on even–even nuclei and they do not give the sign of the quadrupole moment and so cannot distinguish between oblate and prolate shapes. The nuclear re-orientation effect in Coulomb excitation does allow one to determine the shape but it requires a target or a beam of unstable nuclei. Such beams have now become available and are steadily improving in terms of energy, intensity and quality. Nuclear re-orientation will be a very useful tool for future experiments at HIE-ISOLDE.

As the French would say 'revenons a nos moutons'. It turns out that in some cases beta decay provides an alternative way of determining whether the ground state of the parent nucleus is oblate or prolate. The method requires an accurate measurement of the distribution of GT strength, B(GT), as a function of excitation energy in the daughter nucleus. The idea came from Hamamoto and Zhang [48] and was then pursued in more detail by Sarriguren *et al* [49]. In essence the calculations are based on a deformed Hartree–Fock (HF) mean field obtained with a density dependent Skyrme force, such as SG2 or Sk3, including pairing correlations in the BCS approximation. A residual spin-isospin force is introduced consistently and treated in the QRPA. The interested reader will find the details in [50, 51]. The calculations determine low-lying minima in the nuclear potential energy surface (PES) and B (GT) distributions are then calculated for each of these minima on the assumption that the transitions connect states with the same deformation. In some cases the calculated distributions within the beta-decay window differ markedly with the shape of the ground state of the parent nucleus, especially for the light Kr and Sr isotopes and consequently they were the cases we decided to study first.

CERN-ISOLDE is the ideal place to study the beta decays of these nuclei since it provides intense, mass-separated low-energy beams of neutron-deficient Sr and Kr nuclei. We have studied a number of these cases with the *Lucrecia* spectrometer. We do not follow the chronological sequence of the experiments but start with the case of ^{76}Sr [52] where the results are more readily understood. Some previous works suggested that prolate deformation could reach a maximum in this nucleus, therefore it was a good example to test the method. The daughter Rb is much more readily ionised than Sr and would swamp the gamma-ray spectrum for ^{76}Sr. Accordingly a fluorination technique [53], where CF_4 is added to the ion source, was used to produce a clean beam of ^{76}Sr. The F forms a molecule with Sr but not Rb. The half lives of ^{76}Sr and its daughter ^{76}Rb are 7.9 s and 36.8 s, respectively. This is long enough for the activity to be implanted into the tape outside *Lucrecia*. The tape was moved every 15 s to avoid the build up of the ^{76}Rb activity. The data acquisition was inhibited for 10–15 ms after the incoming beam to reduce the background due to neutrons generated in the spallation process in the target. Some characteristics of the experiment are summarised in table 1. The TAS spectrum was recorded in coincidence with positrons and x-rays using the ancillary detectors placed in the through hole in the NaI detector. In this case the analysis was carried out without any condition on the spectra from the ancillary detectors but they were very useful in the on-line control of the experiment. The data were analysed with the methods

Table 1. Some experimental characteristics of the experiments carried out at *Lucrecia* to investigate a series of $N \sim Z$ decaying nuclei. In all cases a proton beam of 1.4 GeV was used. The intensity was controlled by the choice of the number of pulses taken in the super-cycle of the PS-Booster accelerator. It was chosen to produce a counting rate of ~3.5 kHz in *Lucrecia*. It is indicated whether the source is implanted in the tape inside or outside the TAS. This is determined by the half-lives of the nuclei that are involved. They are also shown in the table. The collection and measuring time are given in the final column.

Parent nucl.	Target beam	Ion source	Impl. point inside/outs.	$T_{1/2}$ parent	$T_{1/2}$ daugt.	Cycle
^{76}Sr	Nb(52 mg cm^{-2})	Surf. ion. + fluor.	outside	7.9 s	36.8 s	15 s
^{78}Sr	Nb(52 mg cm^{-2})	Surf. ion. + fluor.	outside	2.6 m	17.7 m	32 s
^{72}Kr	Nb(52 mg cm^{-2})	Plasma + cooled transmission line	inside	17.1 s	78.6 s	15 s
^{74}Kr	Nb(52 mg cm^{-2})	Plasma + cooled transmission line	inside	11.4 m	46 m	25 m

developed by the IFIC group [15–18] that were described earlier. In this case the expectation maximisation algorithm was used to obtain $I_\beta(E)$ by unfolding the experimental data.

Figure 14 shows (a) the experimental total absorption spectrum for ^{76}Sr decay overlaid with the recalculated spectrum after analysis and (b) the B(GT) distribution derived from the resulting analysis. Figure 15 shows the measured accumulated B(GT) as a function of the excitation energy in the daughter nucleus. It is compared with the calculated distributions assuming prolate and oblate shapes. The shading indicates the uncertainty in the experimental distributions. Two minima were found in this case corresponding to $\beta_2 = +0.41$(prolate) and $\beta_2 = -0.13$ (oblate). The calculations shown used the SK3 Skyrme interaction and assume that the parent and daughter states have the same deformation. Other interactions produce very similar results. The generally accepted quenching factor of 0.6 has been applied to the results of the B(GT) calculations. The experimental results agree very well with calculations for a prolate shape over the range 0–5.6 MeV. In contrast the results assuming an oblate shape bear no similarity to experiment. This agrees with a strong deformation of 0.4 deduced from the dynamical properties [54] of the ground state band observed in heavy ion induced fusion-evaporation reactions. It also gives the first definitive evidence that the deformation is prolate.

We turn now to the decay of ^{74}Kr which was measured in a similar way, see [55] and table 1 for details. The cold transmission line strongly suppresses the contamination of noble gas beams by less volatile isobars, such as the Bromine which is directly produced. The contamination was found to be negligible as expected from previous measurements with noble gases. The Br was suppressed by a factor of 10^4. In this case the analysis was carried out with the spectrum in coincidence with Br x-rays. The x-ray spectrum and the gates are shown in figure 2 of the original paper, where we can see clearly, from the fact that there are no Se x-rays visible, that there is no contamination from the daughter decay. The analysis was again carried out as described earlier and figure 15 shows the accumulated $B(GT)$ distribution as a function of excitation energy in the daughter ^{74}Br nucleus. The results are compared with the calculations for $\beta_2 = -0.15$ and $+0.39$, the minima found in the PES in this case with the SG2 interaction. Neither of the two calculated B(GT) strength distributions, assuming pure prolate or oblate shapes, reproduces the experimental B(GT) values over the full range of excitation energy. While the calculation based on an oblate shape is better below 2 MeV, the prolate calculation reproduces the concentration of strength at higher energies.

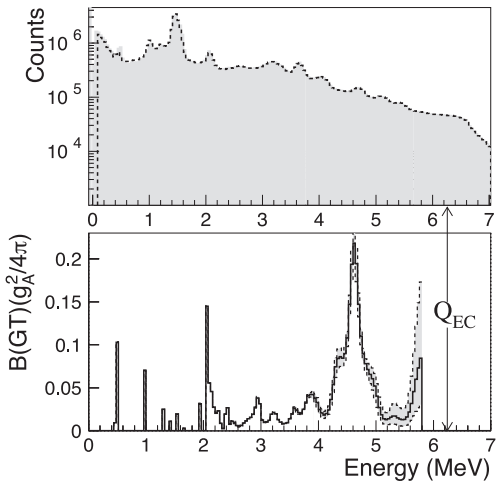

Figure 14. The figure shows (a) the experimental TAS spectrum for ^{76}Sr overlaid with the recalculated spectrum after analysis and (b) the *B*(GT) distribution derived from the analysed spectrum. Reprinted figure with permission from [52], Copyright (2004) by the American Physical Society.

The experimental results systematically lie between the two calculated curves indicating possible shape mixing in the ^{74}Kr ground state. Similar results were obtained if one uses the Sk3 interaction. This result confirms the theoretical predictions of [56] and confirms the evidence from reaction studies [44, 57].

Similar measurements were made for the decay of ^{78}Sr, see table 1 and [37]. The modus operandi was the same as in the other two cases discussed above. As in the other cases it is necessary to determine the spectrum from the daughter nucleus since it has to be subtracted from the spectrum from the parent. In this case there is an added difficulty. There are two states in ^{78}Rb that beta decay with spins and parities 0^+ and 4^-. Both are produced in spallation and cannot be separated. In the beta decay of ^{78}Sr the 4^- state is not populated so the only way to produce the correct background is by producing the ^{78}Rb via the decay of ^{78}Sr. The details of the measurement cycles are given in [37]. In the case of ^{78}Sr decay previous measurements of the decay scheme were limited. Consequently it was necessary to carry out an experiment [58] with Ge detectors to try to improve it. Figure 15 shows the experimental *B*(GT) distribution and compares it with calculated distributions using the SG2, Sk3 and Sly4 Skyrme interactions for the prolate and spherical minima found in the calculations. The conclusion is clear. ^{78}Sr is also prolate in its ground state like its neighbour ^{76}Sr. In this case the decay of ^{78}Rb was also examined in detail. The difficulty here was that no theoretical calculations were available for the decay of this odd–odd nucleus and in consequence the decay of ^{78}Rb was studied in the light of the results obtained for ^{78}Sr. The main conclusion is that the ground state of ^{78}Rb is also prolate. The arguments can be found in [37, 58]. If one looks at these two publications one can find a number of conclusions about the structure of this odd–odd nucleus.

Finally here we turn to the decay of ^{72}Kr. This experiment was carried out immediately after the experiment on ^{74}Kr and the conditions were very similar. The details can be found in [59]. The main difficulty in this measurement was the contamination of the sources with ^{72}As. Moreover, this contaminant was spread out in the tube, and not only at the source location. This is understood to be due to the formation of the As_2 dimer molecule which is volatile and

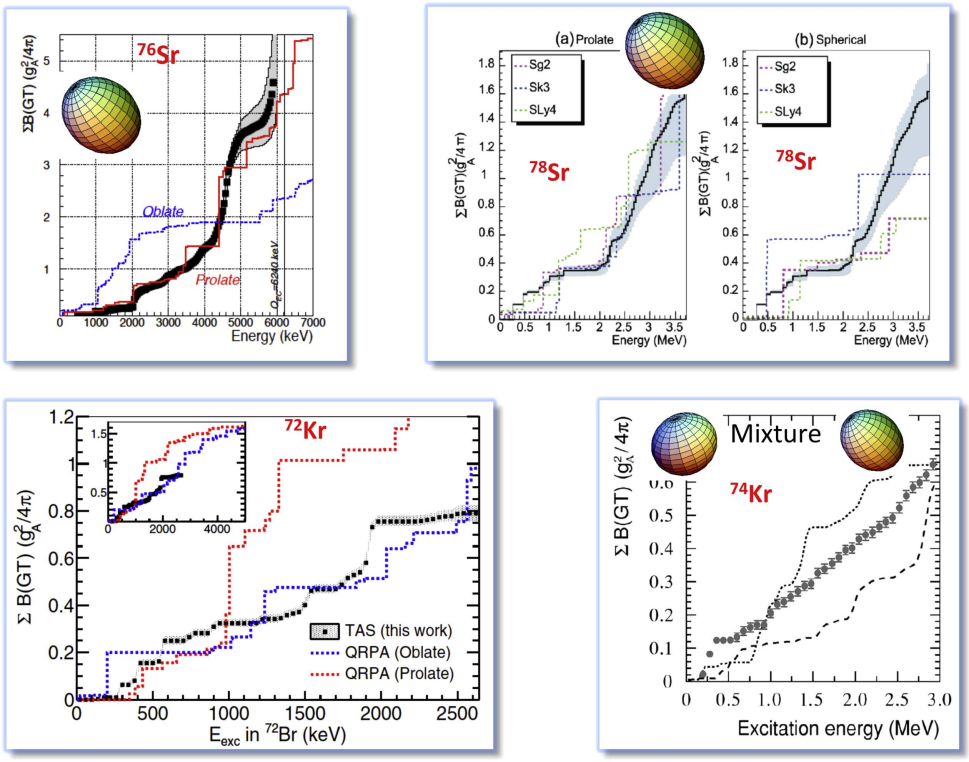

Figure 15. The figure shows the measured accumulated B(GT) value as a function of excitation energy in the daughter nuclei for a number of decays of even–even Sr and Kr nuclei. In the top line from left to right we see the results for ^{76}Sr [52] and ^{78}Sr [37] decay. In the bottom line we see the results for ^{72}Kr [59] and ^{74}Kr [55]. Top left, reprinted figure with permission from [52], Copyright (2004) by the American Physical Society. Top right, reprinted figure with permission from [37], Copyright (2013) by the American Physical Society. Bottom left, reprinted figure with permission from [59], Copyright (2015) by the American Physical Society. Bottom right, reprinted figure with permission from [55], Copyright (2004) by the American Physical Society.

passes through the cold transfer tube but then breaks up at the warmer exit and passes through the mass separator with the Kr since they are close in mass. Since the beta detector lay close to the source it did not 'see' the betas from the spread out contamination. Accordingly in this case only the beta-gated spectra were analysed. The resulting accumulated B(GT) can be seen in figure 16 where the comparison with results from a study with Ge detectors made by Piqueras *et al* [60] is presented. There is clear evidence of the *Pandemonium* effect.

^{72}Kr is a particularly interesting case because some experimental results suggest oblate deformation for this nucleus [61]. This is indeed what we might conclude looking at figure 15 which compares the experimental B(GT) distribution with the results of QRPA calculations using the Sly4 Skyrme interaction for the oblate and prolate minima in the PES found in the calculations. The calculated distributions are very different, with that for the oblate deformation being generally in good agreement with experiment. The prolate distribution reproduces the experimental results up to 1 MeV but beyond that always predicts larger values. Overall the comparison suggests a dominant oblate shape for the ^{72}Kr ground state.

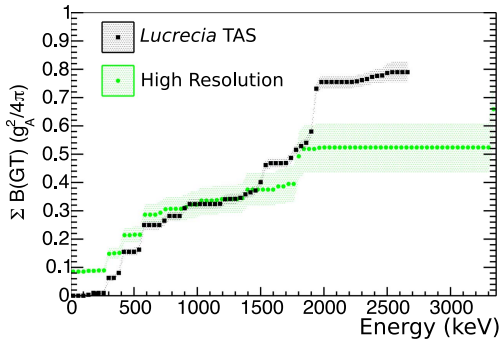

Figure 16. The accumulated B(GT) for the decay of ^{72}Kr as a function of excitation energy measured with Ge detectors [60] and with Lucrecia [59]. The *Pandemonium* effect is shown clearly in this figure. Reprinted figure with permission from [59], Copyright (2015) by the American Physical Society.

The reader should note that in these calculations one cannot mix the two different shapes (this is not an intrinsic difficulty and there are plans to include the effect of mixing configurations in the future). The assumption is that the beta transitions connect states with the same deformation. In consequence an oblate shape with some small admixture of prolate shape cannot be excluded. Interestingly, shell-model calculations, performed in this mass region for the first time, reproduce very nicely the experimental data, see figure 17, while describing the ground state of ^{72}Kr in a different way; as a mixture of oblate and prolate configurations in similar proportions. The calculations assume a ^{56}Ni core and include the $1p_{3/2}$, $0f_{5/2}$, $1p_{1/2}$, $0g_{9/2}$ and $1d_{5/2}$ and the JUN45 interaction described in [62]. The complex excited VAMPIR approach (EXVAM) calculations [63] arrive at similar conclusions. Thus a firm conclusion about the amount of prolate mixing in the ground state is not possible at the moment. However ^{72}Kr is a particularly delicate case for two reasons: firstly because it is an $N = Z$ nucleus, and secondly because there is shape coexistence at very low excitation energy. A second 0^+ state is known at 671 keV energy and even shape mixing in the ground state is plausible. These facts make the calculations very sensitive to small changes in the parameters, and the results are not as robust as in the cases studied earlier. The authors of this work pointed out the importance of a new measurement of this decay over the full energy window as the theoretical models predict different values of the accumulated B(GT) at high excitation energy. As mentioned above this was not possible here because as a consequence of the strong contamination, only the β^+ component of the decay could be studied and consequently the last 1022 keV of the Q-beta window was inaccessible.

The results of this particular work emphasise the importance of obtaining clean sources for TAS measurements both for the parent and descendant activities as well as background spectra with good statistics monitored over the full running time of the experiment.

The examples given earlier focussed on the decays of even–even nuclei but this method of determining nuclear shapes is not confined to them. Measurements have been made with *Lucrecia* of the decay of ^{77}Sr [64]. The analysis was again carried out using the methods developed by the Valencia group. Figure 18 shows the accumulated B(GT) for ^{77}Sr decay compared with the results of HF + BCS + QRPA calculations using several different Skyrme forces for the prolate and spherical minima in the PES found for this nucleus. These results will be published soon.

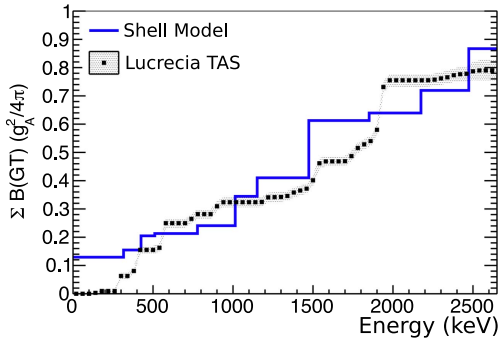

Figure 17. The measured accumulated B(GT) for ^{72}Kr decay as a function of excitation energy, compared with the B(GT) distribution calculated with the shell model. Reprinted figure with permission from [59], Copyright (2015) by the American Physical Society.

3.3. Shape coexistence in the lead nuclei

The shapes of the lead nuclei have been the subject of intense experimental and theoretical interest in recent years. The main reason has been the observation that all of the even–even Pb nuclei with masses $A = 184$–194 have at least one excited 0^+ state below 1 MeV and some, ^{186,188}Pb, have two 0^+ states below 700 keV [66, 67]. This means that they provide an excellent opportunity to study shape effects and shape coexistence [68]. Theoretically the existence of these low-lying excited 0^+ states has been interpreted in terms of the $Z = 82$ shell gap and the large number of neutron holes in the $N = 126$ closed shell. All of these even–even nuclei down to ^{182}Pb are expected to have spherical ground states. Theoretically the coexistence of these 0^+ states has been studied in the framework of a variety of models and this has been summarised in [69]. Theoretical calculations [70, 71] using QRPA predict that the B(GT) distributions for the decays of the even–even Pb nuclei have quite different patterns depending on the deformation of the ground state of the parent nucleus. This was the main motive for the work described here since it represented the opportunity to test this method of comparing the experimental B(GT) with the theoretical calculations in a different mass region. The decays studied with *Lucrecia* were for ^{190,192}Pb. They are of particular interest as test cases since the degree of shape mixing in their ground states is expected to be small [72]. In these experiments the nuclei of interest were produced in the bombardment of a 50 g cm^{-2} target of UCX with a beam of 1.4 GeV protons. The selective laser ion source RILIS [73] was used to enhance the production of Pb ions over the isobaric Tl ions produced in surface ionisation. The general purpose separator was used to separate the ions in mass and after extraction and acceleration to 60 keV they were transported to *Lucrecia*. Two measurements were made for each of the two masses, one with the laser on to produce a beam of predominantly Pb ions and the other with laser off to produce a beam made largely of Tl ions to study contamination. The purities of the mass 192 and 190 Pb ion beams were 96% and 93% respectively with laser on. The half lives are sufficiently long that the ions could be implanted into the tape outside *Lucrecia*. They were then moved in a single step to the measuring point. The measurement cycles were symmetrical collection and measuring times that were adjusted to minimise the contamination from the daughter activities. The measuring times were 4 min for ^{192}Pb and 2 min for ^{190}Pb. The process was repeated until sufficient data were collected. In this case it was possible to analyse the EC component. This is of course the best option if we are to have a very clean spectrum where only the nucleus of interest is present in principle.

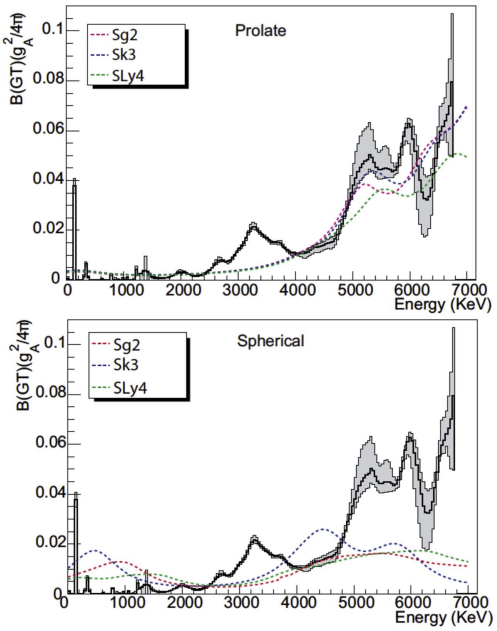

Figure 18. Gamow–Teller strength distribution in the beta-decay of ^{77}Sr as a function of the excitation energy in the daughter nucleus [64]. The upper panel shows the comparison with HF + BCS + QRPA calculations using the Skyrme forces SG2, Sk3 and SLy4 for a prolate shape while the bottom panel panel compares the experimental distribution with the calculations for a spherical shape. A Gaussian of width 1 MeV has been used for the representation of the theoretical calculations [65].

This is not always easy, several conditions have to be fulfilled, namely that we are at the neutron-deficient side of the nuclide table, that we have a strong EC component, and that the x-rays are not contaminated because of strong conversion lines in the daughter nucleus.

The TAS spectra gated with Tl x-rays were analysed using the methods developed by the Valencia group and described earlier. The accumulated B(GT) distributions obtained are compared with the results of QRPA calculations based on the Sly4 interaction [70, 71] in figures 19 and 20. The calculations show spherical, oblate and prolate minima lying close together on the PES. There is more fragmentation of the B(GT) in the deformed cases than in the spherical case, where the strength is concentrated in a single low-lying state, corresponding to the transition from the almost fully occupied proton $h_{11/2}$ orbital to the partly unoccupied neutron $h_{9/2}$ orbital. With this caveat the calculations for the spherical case are in much better agreement than the others as we see in figures 19 and 20. The spherical case also reproduces the total measured strength in the window. The calculations do not include some correlations beyond the mean field. They also ignore the possible configuration mixing of the three shapes. All of the effects not taken into account in the formalism can be effectively included by folding the calculation with a distribution simulating the expected fragmentation. The net effect would be a smoothing of the accumulated B(GT) strength more in accord with observation. Based on the results of the experiments with *Lucrecia* [74] one can infer spherical character for the ground states of ^{190}Pb and ^{192}Pb. This provides an additional and independent proof of the results of [75], where small deviations from the Liquid Drop Model

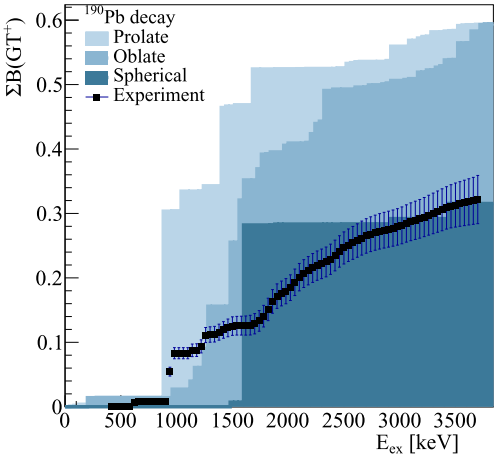

Figure 19. The measured accumulated B(GT) as a function of excitation in the daughter nucleus for the beta decays of ^{190}Pb. The experimental result is compared with the results of calculations for prolate, oblate and spherical shapes of the parent nuclei. Reprinted figure with permission from [74], Copyright (2015) by the American Physical Society.

for these nuclei were interpreted as being the effect of small admixtures of intruder configurations in the ground state wave functions.

3.4. Future measurements

There are many possible future experiments that can be carried out with *Lucrecia* at ISOLDE. Measurements of the B(GT) distribution in β decay provide stringent tests of nuclear model calculations. They have been neglected in the past because there was no reliable means of measuring such distributions accurately. Now that spectrometers with physical dimensions approaching the ideal 4π detector for total absorption spectroscopy are available and the IFIC group have put the analysis of the data from TAS spectrometers on a sound and reliable footing [15–18] there are many cases that can be studied at ISOLDE and elsewhere. The Valencia–Surrey–Madrid collaboration have already carried out further measurements [76] on the shapes of the even–even Hg nuclei, encouraged by the results described above on the Pb isotopes. Again theoretical calculations [70, 71] show clear differences between the B(GT) distributions depending on the deformation of the ground states of the parent nuclei. The analysis is ongoing.

Overall the prolate case is in better agreement since the spherical minimum calculations predict a lot of strength at low energies and fall well below the total accumulated strength up to the Q window cut-off. This indication of prolate deformation is consistent with an earlier measurement [77] of the quadrupole moment.

In the introduction to this article it was pointed out that accurate measurements of B(GT) distributions for the β decays of fission products are important for a number of reasons including the need to have a good knowledge of reactor decay heat. TAS is the ideal way to provide such information and already Algora *et al* [78] have solved a known discrepancy in the reactor decay heat for the fission of ^{239}Pu in the 4–3000 s cooling period using the Russian TAgS at Jyväskylä. More such measurements are required and, since ISOLDE can provide good beams of some fission fragments, we expect that some of them will be made with

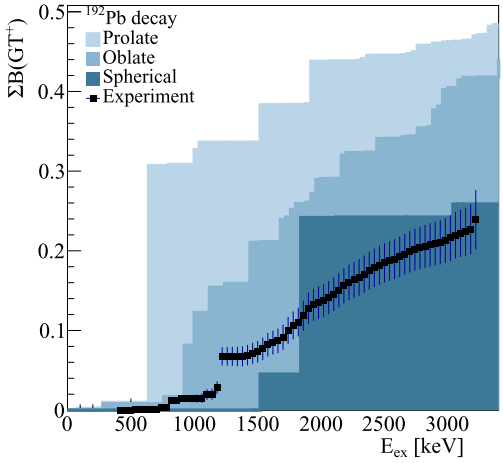

Figure 20. The measured accumulated B(GT) as a function of excitation in the daughter nucleus for the beta decays of ^{192}Pb. The experimental result is compared with the results of calculations for prolate, oblate and spherical shapes of the parent nuclei. Reprinted figure with permission from [74], Copyright (2015) by the American Physical Society.

Lucrecia. It should be noted, however, that such measurements need very clean sources and they are more difficult to produce on the neutron-rich side of stability. Indeed until now this type of measurement has been carried out at Jyväskylä using the double Penning trap as a purification device [32].

Beta decays and the Weak interaction play a major role in many explosive astrophysical events. For example nucleosynthesis occurs in explosive hydrogen burning at high T (T greater than 10^8 K) and is characterised by the astrophysical rp-process. It is thought that the extreme conditions involved occur in Type 1 x-ray bursts. This occurs in binary systems consisting of a neutron star and a red giant or main sequence star. Material is dragged from the star on to the surface of the neutron star where the pressure and temperature builds up until thermonuclear runaway occurs. Thermonuclear ignition occurs when the pressure and temperature build up in the accreted envelope to the point where breakout occurs from the CNO cycle. Nucleosynthesis now proceeds near the proton drip-line via the rp-process. Type-1 x-ray bursters are characterised by $T_{\rm peak}$ approximately 1–3 GK and rho equal to 10^6–10^9 g cm^{-3}. They reach peak luminosities of 10^{39} ergs per second in timescales from 3 to 1000 s. An up-to-date summary can be found in [79]. In this scenario the rp-process follows a series of rapid proton captures as long as the proton capture rates are orders-of-magnitude faster than the competing β decays. As the pathway approaches the proton drip-line strong photodisintegration sets in and pure proton decay occurs as well. Now the reaction flow has to wait until the much slower beta decay can occur. The nuclei where this occurs are known as waiting points (WP) since the overall timescale is of the order of 100 s any delay for a β decay of several seconds will considerably influence all the physical observables such as the nuclear energy production rate which translates into the luminosity curve. This is the main quantity that models can try to reproduce and consequently a knowledge of the decay rates of the WP nuclei and their neighbours on the Segre Chart is important. No x-ray Burster model has yet included all the electron capture contributions to the rp-process pathway. The reason is

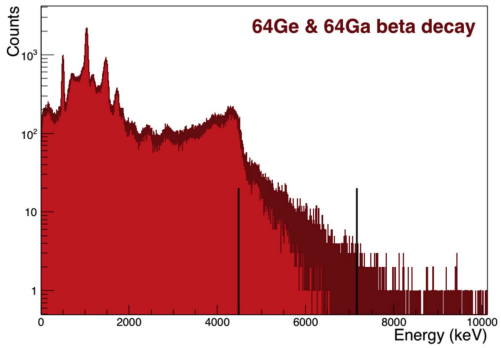

Figure 21. The figure shows the spectrum from the decay of ^{64}Ge and its daughter ^{64}Ga measured with *Lucrecia*.

because under the extreme conditions involved the atoms are completely ionised and so the electron capture occurs with continuum electrons (cEC). Reference [80] showed, followed by [81], that cEC plays an important role in the weak interaction rates of nuclei close to the proton drip-line in x-ray burster calculations. [82] asserts that precise measurements of beta decay distributions for the WP nuclei are necessary to validate calculations of the cEC processes. Accordingly a campaign of measurements of ^{64,66}Ge and ^{66,68}Se was accepted as a proposal at ISOLDE and measurements with *Lucrecia* for the Ge nuclei have already been carried out [83]. The resulting raw *Lucrecia* spectrum for ^{64}Ge and its daughter ^{64}Ga are shown in figure 21. At the time of writing, the data are being analysed. Measurements on the ^{66,68}Se isotopes and other nuclei of astrophysical interest will follow.

As indicated earlier B(GT) distributions can provide a vital testing ground for nuclear structure calculations and accurately measured distributions are also of importance to ensure that the information in international nuclear databases can be used for reactor decay heat and reactor antineutrino spectrum calculations with confidence. We anticipate many TAS measurements will be carried out in future with *Lucrecia* and the new generation of TAS spectrometers. As the advertisers would say 'watch this space'.

Acknowledgments

This work has been supported by the Spanish Ministerio de Economia y Competitividad under the FPA 2014-52823-C2-1-P, the AIC-A-2011-0696 and the SEV-2014-0398 grants, by the European Commission under the FP7/EURATOM contract 602503 and by the Spanish Ministerio de Educacion under the FPU12/01527 grant. IFIC is a centre of excellence Severo Ochoa. It was also supported by the Science and Technology facilities Council UK under grant No. ST/FO12012/1. WG acknowledges the support of the University of Valencia. The initial setting up of *Lucrecia* and the design and building of the shielding was carried out in a collaboration between IFIC-Valencia, University of Surrey, IRES-Strasbourg and IEM-Madrid. The authors would like to acknowledge the contributions of the people, particularly Ph. Dessagne and his group, who took part in the construction of the shielding and the β detector.

References

[1] Nichols A L 2000 Nuclear data requirements for decay heat calculations *Proc. Frederic Joliot/Otto Hahn School in Reactor Physics (CEA Cadarache, Cadarache, France)* p 211 and references therein
[2] Abe Y *et al* 2012 *Phys. Rev. Lett.* **108** 0131801
[3] An F P *et al* 2012 *Phys. Rev. Lett.* **108** 071803
[4] Ahn J K *et al* 2012 *Phys. Rev. Lett.* **108** 191802
[5] Christensen E *et al* 2014 *Phys. Rev. Lett.* **113** 042503
[6] Hardy J C, Carraz L C, Jonson B and Hansen P G 1977 *Phys. Lett.* B **71** 307
[7] Duke C L *et al* 1970 *Nucl. Phys.* A **151** 609
[8] Johansen K H, Bonde Nielsen K and Rudstam G 1973 *Nucl. Phys.* A **203** 481
[9] Firestone R B *et al* 1982 *Phys. Rev.* C **25** 527
[10] Alkhazov G D *et al* 1985 *Phys. Lett.* B **157** 35
[11] Greenwood R C *et al* 1992 *Nucl. Instrum. Methods* A **314** 514
[12] Guadilla V *et al* 2017 *Acta Phys. Pol.* B **48** 529
[13] Karny M *et al* 1997 *Nucl. Instrum. Methods* B **126** 411
[14] Nacher E *et al* 2016 *Phys. Rev.* C **93** 014308
[15] Tain J L and Cano-Ott D 2007 *Nucl. Instrum. Methods* A **571** 719
[16] Tain J L and Cano-Ott D 2007 *Nucl. Instrum. Methods* A **571** 728
[17] Cano-Ott D *et al* 1999 *Nucl. Instrum. Methods* A **430** 333
[18] Cano-Ott D *et al* 1999 *Nucl. Instrum. Methods* A **430** 488
[19] Algora A *et al* 2003 *Phys. Rev.* C **68** 034301
[20] Hu Z *et al* 1998 *Nucl. Instrum. Methods* A **419** 121
[21] Eberth J *et al* 1996 *Nucl. Instrum. Methods* A **369** 135
[22] Hu Z *et al* 2000 *Phys. Rev.* C **62** 064315
Karny M *et al* 2001 *Nucl. Phys.* A **690** 367
Gierlik M *et al* 2003 *Nucl. Phys.* A **724** 313
[23] Zakari-Issafou A A *et al* 2015 *Phys. Rev. Lett.* **115** 102503
[24] Algora A *et al* 2014 *Nucl. Data Sheets* **120** 12
[25] Valencia E *et al* 2017 *Phys. Rev.* C **95** 024320
[26] Tain J L *et al* 2015 *Nucl. Instrum. Methods* A **803** 36
[27] Rubio B 2006 *Int. J. Mod. Phys.* E **15** 1979
[28] Davinson T *et al* 2017 *JPS Conf. Proc.* **14** 020622
[29] Winkler M *et al* 2008 *Nucl. Instrum. Methods* B **266** 4192
[30] Kubo T *et al* 2003 *Nucl. Instrum. Methods* B **204** 97
Kubo T *et al* 2012 *Prog. Theor. Exp. Phys.* **2012** 03C003
[31] Guadilla V *et al* 2016 *Nucl. Instrum. Methods* A **376** 334
[32] Aysto J 2001 *Nucl. Phys.* A **693** 477
Eronen T *et al* 2012 *Eur. Phys. J.* A **48** 46
[33] Quinn S J *et al* 2014 *Nucl. Instrum. Methods* A **757** 62
[34] Spyrou A *et al* 2016 *Phys. Rev. Lett.* **117** 142701
Dombos A C *et al* 2016 *Phys. Rev.* C **93** 064317
[35] Wolinska-Cichoka M *et al* 2014 *Nucl. Data Sheets* **120** 22
[36] Rasco B C *et al* 2015 *Nucl. Instrum. Methods* A **788** 137
[37] Perez-Cerdan A *et al* 2013 *Phys. Rev.* C **88** 014324
[38] Rubio B *et al* 2005 *J. Phys. G: Nucl. Part. Phys.* **31** S1477
[39] Rubio B and Gelletly W 2009 Beta decay of exotic nuclei *The Euroschool Lectures on Physics with Exotic beams Vol III* (*Springer Lecture Notes in Physics* vol 764) ed J S Al-Khalili and E Roeckl (Berlin: Springer) p 99
[40] Ahmad I and Butler P A 1993 *Ann. Rev. Nucl. Part. Sci.* **43** 71
Butler P A and Nazarewicz W 1996 *Rev. Mod. Phys.* **68** 349
[41] Nazarewicz W *et al* 1985 *Nucl. Phys.* A **435** 397
[42] Bonche P *et al* 1985 *Nucl. Phys.* A **443** 39
[43] Hamilton J H *et al* 1974 *Phys. Rev. Lett.* **32** 239
[44] Chandler C *et al* 1997 *Phys. Rev.* C **56** R2924

[45] Neugart R and Neyens G 2006 Nuclear moments *The Euroschool Lectures on Physics with Exotic beams Vol II* (*Springer Lecture Notes in Physics* vol 700) ed J S Al-Khalili and E Roeckl (Berlin: Springer) p 135
[46] Davni E *et al* 1983 *Phys. Rev. Lett.* **50** 1652
[47] Hardeman F *et al* 1991 *Phys. Rev.* C **43** 130
[48] Hamamoto I and Zhang X Z 1995 *Z. Phys.* A **353** 145
[49] Sarriguren P *et al* 2001 *Nucl. Phys.* A **691** 631
[50] Sarriguren P *et al* 1998 *Nucl. Phys.* A **635** 55
[51] Sarriguren P *et al* 1999 *Nucl. Phys.* A **658** 13
[52] Nacher E *et al* 2004 *Phys. Rev. Lett.* **92** 232501
[53] Ravn H L *et al* 1975 *Nucl. Instrum. Methods* A **123** 131
[54] Lister C J *et al* 1990 *Phys. Rev.* C **42** R1191
[55] Poirier E *et al* 2004 *Phys. Rev.* C **69** 034307
[56] Petrovici A, Schmid A and Faessler A 2000 *Nucl. Phys.* A **665** 333
[57] Becker F *et al* 1999 *Eur. Phys. J* A **4** 103
[58] Perez-Cerdan A *et al* 2011 *Phys. Rev.* C **84** 054311
[59] Briz J A *et al* 2015 *Phys. Rev.* C **92** 054326
[60] Piqueras I *et al* 2003 *Eur. Phys. J* A **16** 313
[61] Bouchez E *et al* 2003 *Phys. Rev. Lett.* **90** 082502
[62] Honma M *et al* 2009 *Phys. Rev.* C **80** 064323
[63] Petrovici A, Schmid A and Faessler A 2008 *Phys. Rev.* C **78** 044315
[64] Perez-Cerdan A B 2012 *PhD Thesis* University of Valencia
[65] Sarriguren P 2012 private communication
[66] Andreyev A N *et al* 2000 *Nature* **405** 430
[67] Heese J *et al* 1993 *Phys. Lett.* B **302** 390
[68] Julin R, Helariutta K and Muikko M 2001 *J. Phys. G: Nucl. Part. Phys.* **27** R109
[69] Heyde K and Wood J L 2011 *Rev. Mod. Phys.* **83** 167
[70] Sarriguren P *et al* 2005 *Phys. Rev.* C **72** 054317
[71] Moreno O *et al* 2006 *Phys. Rev.* C **73** 054302
[72] Fossion R *et al* 2003 *Phys. Rev.* C **67** 024306
[73] Mishin V *et al* 1993 *Nucl. Instrum. Methods* B **73** 550
[74] Estevez Aguado M E *et al* 2015 *Phys. Rev.* C **92** 044321
[75] De Witte H *et al* 2007 *Phys. Rev. Lett.* **98** 112502
[76] Algora A, Fraile L M and Nacher E ISOLDE experiment IS539 Shape effects in the vicinity of the $Z = 82$ line: study of the beta decay of ^{182,184,186}Hg
[77] Lievens P 1992 *Phys. Rev.* C **46** 707
[78] Algora A *et al* 2010 *Phys. Rev. Lett.* **105** 202501
[79] Parikh A *et al* 2013 *Prog. Part. Nucl. Phys.* **69** 225
[80] Sarriguren P 2009 *Phys. Lett.* B **680** 438
[81] Jameel-Un N 2012 *Astrophys. Space Sci.* **339** 305
[82] Sarriguren P 2011 *Phys. Rev.* C **83** 025801
[83] Nacher E, Domingo-Pardo C and Algora A ISOLDE experiment IS570 Beta decay of the $N = Z$, rp-process waiting points: ^{64}Ge, ^{68}Se and the $N = Z + 2$: ^{66}Ge, ^{70}Se for accurate stellar weak-decay rates